

## Photocatalytic Formation of I–I Bonds Using DNA Which Enables Detection of Single Nucleotide Polymorphisms

Kiyohiko Kawai,\* Haruka Kodera, and Tetsuro Majima\*

*The Institute of Scientific and Industrial Research (SANKEN), Osaka University, Mihogaoka 8-1, Ibaraki, Osaka 567-0047, Japan*

Received July 2, 2010; E-mail: kiyohiko@sanken.osaka-u.ac.jp; majima@sanken.osaka-u.ac.jp

**Abstract:** By decreasing the HOMO energy gap between the base-pairs to increase the charge conductivity of DNA, the positive charge photochemically generated in DNA can be made to migrate along the  $\pi$ -way of DNA over long distances to form a long-lived charge-separated state. By fine-tuning the kinetics of the charge-transfer reactions, we designed a functionalized DNA system in which absorbed photon energy is converted into chemical energy to form I–I covalent bonds, where more than 100 I<sub>2</sub> molecules were produced per functionalized DNA. Utilizing the fact that charge-transfer kinetics through DNA is sensitive to the presence of a single mismatch that causes the perturbation of the  $\pi$ -stacks, single nucleotide polymorphisms (SNPs) in genomic sequences were detected by measuring the photon energy conversion efficiency in DNA by a conventional starch iodine method.

### Introduction

It was not long after Watson and Crick solved the structure of DNA that the array of stacked aromatic bases was suggested to serve as a pathway for charge migration.<sup>1</sup> Recent advances in DNA nanotechnology allow us to construct various nanometer-sized two- and three-dimensional structures,<sup>2–5</sup> and thus, DNA has attracted wide attention as a promising building block for nanoelectronic sensors and photoenergy conversion devices.<sup>6–8</sup> Extensive studies based on polyacrylamide gel electrophoresis strand cleavage experiments carried out over the past two decades have clearly demonstrated that a positive charge does in fact migrate along DNA over hundreds of angstroms.<sup>9–15</sup> However, at the same time, it has been shown that the charge-transfer rate is not fast enough to fully compete with the oxidative degradation of DNA, which has hampered the use of

DNA as the path of the positive charge. Theoretical<sup>16–18</sup> and kinetic<sup>19–25</sup> studies of charge transfer in DNA have demonstrated that the low conductivity of DNA is mainly due to the large HOMO energy gap between the two types of base-pairs, G-C and A-T. We recently found that the charge-transfer efficiency through DNA can be dramatically increased by replacing A with its analogue 7-deazaadenine<sup>26</sup> or diaminopurine (D),<sup>27</sup> both of which have HOMO levels closer to that of G without disturbing the complementary base-pairing. In particular, D can fully replace A during PCR and thus can be used to construct DNA with increased CT efficiency by PCR amplification of DNA sequences of interest.<sup>28</sup> In this study, by using DNA in which the A-T base-pairs were replaced with D-T base-pairs in order to achieve a high charge-transfer efficiency, we established a functionalized DNA system which can convert

- (1) Eley, D. D.; Spivey, D. I. *Trans. Faraday Soc.* **1962**, *58*, 411.
- (2) Liao, S.; Seeman, N. C. *Science* **2004**, *306*, 2072.
- (3) Rothmund, P. W. K. *Nature* **2006**, *440*, 297.
- (4) Andersen, E. S.; Dong, M.; Nielsen, M. M.; Jahn, K.; Subramani, R.; Mamdouh, W.; Golas, M. M.; Sander, B.; Stark, H.; Oliveira, C. L. P.; Pedersen, J. S.; Birkedal, V.; Besenbacher, F.; Gothelf, K. V.; Kjems, J. *Nature* **2009**, *459*, 73.
- (5) Endo, M.; Katsuda, Y.; Hidaka, K.; Sugiyama, H. *J. Am. Chem. Soc.* **2010**, *132*, 1592.
- (6) Cohen, H.; Noguees, C.; Naaman, R.; Porath, D. *Proc. Natl. Acad. Sci. U.S.A.* **2005**, *102*, 11589.
- (7) Hihath, J.; Xu, B.; Zhang, P.; Tao, N. *Proc. Natl. Acad. Sci. U.S.A.* **2005**, *102*, 16979.
- (8) Guo, X.; Gorodetsky, A. A.; Hone, J.; Barton, J. K.; Nuckolls, C. *Nat. Nanotechnol.* **2008**, *3*, 163.
- (9) Meggers, E.; Michel-Beyerle, M. E.; Giese, B. *J. Am. Chem. Soc.* **1998**, *120*, 12950.
- (10) Henderson, P. T.; Jones, D.; Hampikian, G.; Kan, Y. Z.; Schuster, G. B. *Proc. Natl. Acad. Sci. U.S.A.* **1999**, *96*, 8353.
- (11) Nunez, M. E.; Hall, D. B.; Barton, J. K. *Chem. Biol.* **1999**, *6*, 85.
- (12) Nakatani, K.; Dohno, C.; Saito, I. *J. Am. Chem. Soc.* **1999**, *121*, 10854.
- (13) Giese, B.; Amaudrut, J.; Kohler, A. K.; Spormann, M.; Wessely, S. *Nature* **2001**, *412*, 318.
- (14) Kanvah, S.; Joseph, J.; Schuster, G. B.; Barnett, R. N.; Cleveland, C. L.; Landman, U. *Acc. Chem. Res.* **2010**, *43*, 280.
- (15) Genereux, J. C.; Barton, J. K. *Chem. Rev.* **2010**, *110*, 1642.
- (16) Bixon, M.; Giese, B.; Wessely, S.; Langenbacher, T.; Michel-Beyerle, M. E.; Jortner, J. *Proc. Natl. Acad. Sci. U.S.A.* **1999**, *96*, 11713.
- (17) Jortner, J.; Bixon, M.; Voityuk, A. A.; Roesch, N. *J. Phys. Chem. A* **2002**, *106*, 7599.
- (18) Voityuk, A. A.; Roesch, N. *J. Phys. Chem. B* **2002**, *106*, 3013.
- (19) Lewis, F. D.; Liu, X. Y.; Liu, J. Q.; Miller, S. E.; Hayes, R. T.; Wasielewski, M. R. *Nature* **2000**, *406*, 51.
- (20) Lewis, F. D.; Liu, J.; Weigel, W.; Rettig, W.; Kurnikov, I. V.; Beratan, D. N. *Proc. Natl. Acad. Sci. U.S.A.* **2002**, *99*, 12536.
- (21) Lewis, F. D.; Liu, J.; Zuo, X.; Hayes, R. T.; Wasielewski, M. R. *J. Am. Chem. Soc.* **2003**, *125*, 4850.
- (22) Vura-Weis, J.; Wasielewski, M. R.; Thazhathveetil, A. K.; Lewis, F. D. *J. Am. Chem. Soc.* **2009**, *131*, 9722.
- (23) Takada, T.; Kawai, K.; Fujitsuka, M.; Majima, T. *Proc. Natl. Acad. Sci. U.S.A.* **2004**, *101*, 14002.
- (24) Takada, T.; Kawai, K.; Fujitsuka, M.; Majima, T. *Chem.—Eur. J.* **2005**, *11*, 3835.
- (25) Osakada, Y.; Kawai, K.; Fujitsuka, M.; Majima, T. *Nucleic Acids Res.* **2008**, *36*, 5562.
- (26) Kawai, K.; Kodera, H.; Osakada, Y.; Majima, T. *Nat. Chem.* **2009**, *1*, 156.
- (27) Kawai, K.; Kodera, H.; Majima, T. *J. Am. Chem. Soc.* **2010**, *132*, 627.
- (28) Suspene, R.; Renard, M.; Henry, M.; Guetard, D.; Puyraimond-Zemmour, D.; Billecocq, A.; Bouloy, M.; Tangy, F.; Vartanian, J.-P.; Wain-Hobson, S. *Nucleic Acids Res.* **2008**, *36*, e72/1.

the absorbed photon energy to produce  $I_2$ . A photoinduced charge-separated state was generated in the genomic DNA sequences containing single nucleotide polymorphisms (SNPs), where the presence of a mismatch causes the perturbation of the  $\pi$ -stacks, resulting in a decrease of charge-transfer efficiency and subsequent charge-separation yield.<sup>7,25,29–32</sup> The absorbed photon-energy was used to catalytically oxidize iodide ion with the aid of superoxide dismutase (SOD) to ultimately produce  $I_2$ , which enabled the detection of SNPs in the genomic DNA sequence using the well-known iodine–starch reaction.

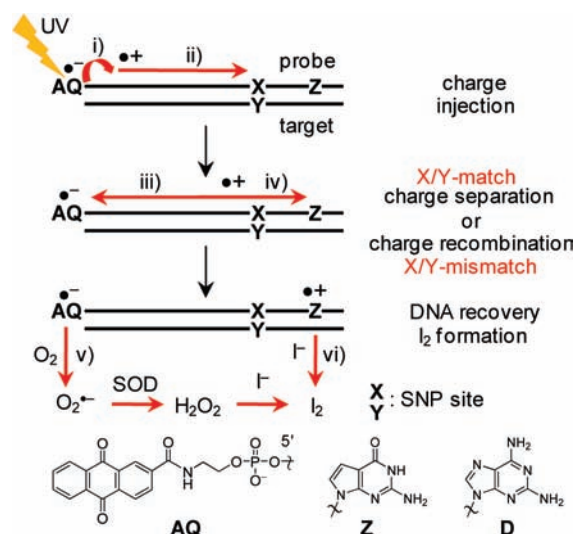
## Experimental Section

**Laser Flash Photolysis.** The nanosecond transient absorption measurements were performed using the laser flash photolysis technique.<sup>23–27,33–37</sup> Briefly, the third-harmonic oscillation (355 nm, fwhm of 4 ns, 8 mJ/pulse) from a Q-switched Nd:YAG laser (Continuum, Surelight) was used for the excitation light which was expanded to a 1-cm diameter. The light from a xenon flash lamp (Osram, XBO-450) was focused into the sample solution for the transient absorption measurement. Time profiles of the transient absorption in the UV–visible region were measured with a monochromator (Nikon, G250) equipped with a photomultiplier (Hamamatsu Photonics, R928) and digital oscilloscope (Tektronics, TDS-580D). The time profiles were obtained from the average of 32 laser shots.

**Iodine–starch Reaction.** Photoirradiation was carried out in an aqueous solution containing 1  $\mu$ M DNA (strand conc.), 10  $\mu$ M SOD (Roche), 50 mM KI, 0.25% starch, and 10 mM pH 7.0 Na phosphate buffer. Solution mixture was photoirradiated with a mercury lamp (Asahi Spectra REX-120) equipped with 340 nm filter (0.6 W/cm<sup>2</sup>) for 1 to 150 min.

**PCR.** PCR on rs965513 DNA (5'-AACAGATCAAAA-A/G-GAGTAAATTA AAAAGAAGATGTATTAGT/3'-TTGTCTAGTTT-T/C-CTCATTTAATTTTCTTCTACATAATCA) was performed with a forward primer 5'-AACAGATCAAAA (primer-1) and a reverse primer 3'-TCTACATAATCA (primer-2). The amplification reaction was carried out with 0.1  $\mu$ M of primer-1, 40  $\mu$ M of primer-2, 0.4 mM of dNTPs (dDTP (TriLink Bio Tech.), dTTP, dCTP, dGTP (Roche)), PrimeSTAR HS DNA Polymerase (Takara), and rs965513 DNA (0.2  $\mu$ g) in a final volume of 500  $\mu$ L. The amplification protocol was 98 °C for 2 min, and 20 cycles of 98 °C for 10 s, 30 °C for 15 s, and 72 °C for 10 s on PCR Thermal Cycler (iCycler Bio-Rad). PCR products were analyzed by native agarose gel (3.5% agarose gel, stained by SYBR green). Fluorescence intensities of PCR solutions after certain cycles were monitored with a transilluminator (LMS-20E UVP) (Figure S3 in Supporting Information). For the iodine–starch reaction, the PCR amplicon was desalted using the spin column (QIAquick Nucleotide Removal Kit, Qiagen), and SOD (20  $\mu$ M), starch (0.1%), KI (20 mM), and probe strand **II-pA** or **II-pG** (1  $\mu$ M) were added. Solution

**Scheme 1.** Kinetic Scheme for Photocatalytic Production of  $I_2$  Using the Functionalized DNA



mixture was photoirradiated with a mercury lamp (Asahi Spectra REX-120) equipped with 340 nm filter (0.07 W/cm<sup>2</sup>) for 150 min at 0 °C.

## Results

The strategy for the photocatalytic production of  $I_2$  using the functionalized DNA is schematically shown in Scheme 1. Anthraquinone (AQ) was attached as a photosensitizer at the 5' end of the probe strand in order to inject a positive charge into the DNA upon UV irradiation (<1 ps) while forming the radical anion of AQ ( $AQ^{\bullet-}$ ) (i).<sup>14,32,38–40</sup> The injected positive charge migrates along DNA (ii) while competing with the charge recombination (iii). When the probe hybridizes with the target strand that causes a mismatch at the SNP site, it acts as a barrier to the migration of a positive charge, which results in the charge recombination (iii). On the other hand, a positive charge can migrate across the SNP site in the case of a matched duplex to be trapped at deazaguanine (Z) and to form a radical cation of Z ( $Z^{\bullet+}$ ), producing a long-lived charge-separated state (iv). Formation of the long-lived charge-separated state allows the reaction of  $AQ^{\bullet-}$  with molecular oxygen ( $O_2$ ) to take place<sup>39</sup> with a time constant of  $\tau_{O_2} = 4.7 \mu$ s (under air-saturated condition) to form a superoxide ( $O_2^{\bullet-}$ ) while recovering AQ (v) (see Supporting Information Figure S1). We used SOD to convert  $O_2^{\bullet-}$  to  $H_2O_2$ , which oxidizes the iodide ion ( $I^-$ ) to produce  $I_2$ . At the same time,  $Z^{\bullet+}$  ( $E_{rdx} = 0.98$  V vs NHE)<sup>41,42</sup> also oxidizes  $I^-$  ( $E_{rdx} = 0.54$  V vs NHE)<sup>43</sup> to produce  $I_2$  and reproduce Z with a time constant of about 20  $\mu$ s (vi) (see Supporting Information Figure S2). Thus, the functionalized matched DNA can catalytically produce  $I_2$  upon photoirradiation, and the SNPs can be detected by monitoring the yield of  $I_2$  based on the starch–iodine reaction.

- (29) Boon, E. M.; Ceres, D. M.; Drummond, T. G.; Hill, M. G.; Barton, J. K. *Nat. Biotechnol.* **2000**, *18*, 1096.  
 (30) Bhattacharya, P. K.; Barton, J. K. *J. Am. Chem. Soc.* **2001**, *123*, 8649.  
 (31) Okamoto, A.; Kamei, T.; Saito, I. *J. Am. Chem. Soc.* **2006**, *128*, 658.  
 (32) Schlientz, N. W.; Schuster, G. B. *J. Am. Chem. Soc.* **2003**, *125*, 15732.  
 (33) Osakada, Y.; Kawai, K.; Fujitsuka, M.; Majima, T. *Proc. Natl. Acad. Sci. U.S.A.* **2006**, *103*, 18072.  
 (34) Kawai, K.; Osakada, Y.; Fujitsuka, M.; Majima, T. *Chem. Biol.* **2005**, *12*, 1049.  
 (35) Kawai, K.; Osakada, Y.; Takada, T.; Fujitsuka, M.; Majima, T. *J. Am. Chem. Soc.* **2004**, *126*, 12843.  
 (36) Kawai, K.; Takada, T.; Tojo, S.; Majima, T. *J. Am. Chem. Soc.* **2003**, *125*, 6842.  
 (37) Kawai, K.; Takada, T.; Nagai, T.; Cai, X.; Sugimoto, A.; Fujitsuka, M.; Majima, T. *J. Am. Chem. Soc.* **2003**, *125*, 16198.

- (38) Armitage, B.; Yu, C.; Devadoss, C.; Schuster, G. B. *J. Am. Chem. Soc.* **1994**, *116*, 9847.  
 (39) Sani, L.; Schuster, G. B. *J. Am. Chem. Soc.* **2000**, *122*, 11545.  
 (40) Lewis, F. D.; Thazhathveetil, A. K.; Zeidan, T. A.; Vura-Weis, J.; Wasielewski, M. R. *J. Am. Chem. Soc.* **2010**, *132*, 444.  
 (41) Nakatani, K.; Dohno, C.; Saito, I. *J. Am. Chem. Soc.* **2000**, *122*, 5893.  
 (42) Dohno, C.; Saito, I. In *Charge Transfer in DNA*; Wagenknecht, H.-A., Eds.; Wiley-VCH: Weinheim, 2005; p 153.  
 (43) Gardner, J. M.; Abrahamsson, M.; Farnum, B. H.; Meyer, G. J. *J. Am. Chem. Soc.* **2009**, *131*, 16206.

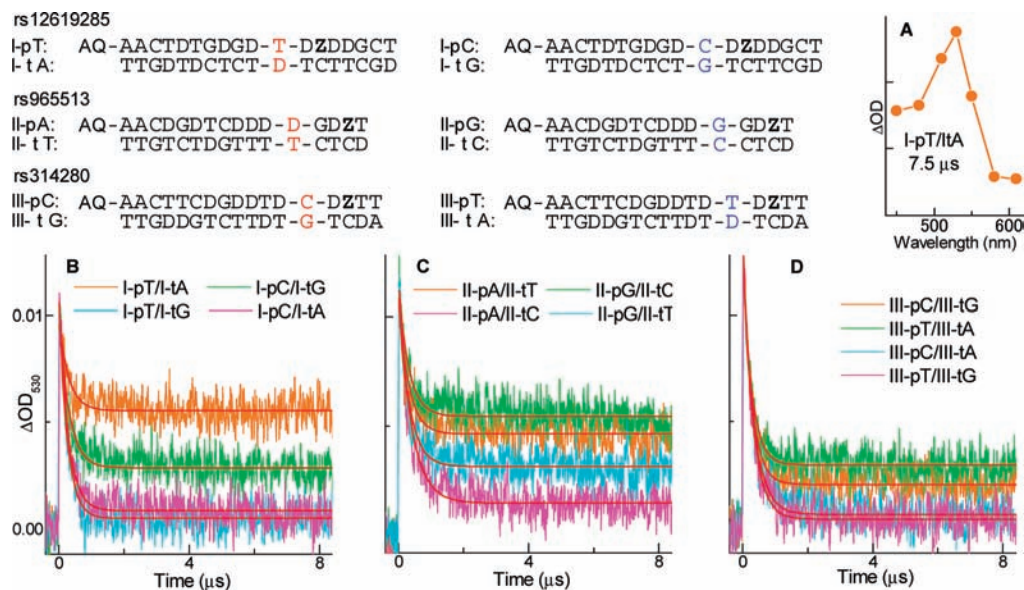


**Figure 1.** Kinetic investigation of the charge-injection, charge-recombination, and charge-transfer processes in the three genomic DNA sequences. (A) The transient absorption spectrum of  $AQ^{\bullet+}$  obtained at  $7.5 \mu s$  after the 355-nm laser flash excitation of **I-pT/I-tA**. (B–D) Time profiles of the transient absorption of  $AQ^{\bullet+}$  monitored at 530 nm during the laser flash photolysis of the target and probe combinations investigated for (B) rs12619285, (C) rs965513, and (D) rs314280. A long-lived charge-separated state was formed for the probe and target combinations that formed a matched duplex (orange and green). On the other hand, the  $AQ^{\bullet+}$  rapidly decayed for probe and target combinations that formed a mismatch (cyan and red violet). The smoothed red curves superimposed on the experimental data are the single exponential fit from which the charge-recombination rate ( $1/\tau$ ) and charge-separation yield of the long-lived charge-separated state monitored at  $5 \mu s$  ( $\Phi_{5\mu s}$ ) were determined. The sample aqueous solution contained  $50 \mu M$  DNA in 10 mM Na phosphate buffer (pH 7.0). The oxygen was removed by purging with Ar to prevent the reaction between  $AQ^{\bullet+}$  and  $O_2$ .

The above-described photocatalytic  $I_2$  production chemistry was examined for three genomic DNA sequences recently revealed to be associated with asthma and myocardial infarction (rs12619285: **I-(A/G)**),<sup>44</sup> thyroid cancer (rs965513: **II-(T/C)**),<sup>45</sup> and breast, ovarian, and endometrial cancers (rs314280: **III-(G/A)**).<sup>46</sup> Two probe sequences were synthesized for each of the three SNP-containing DNA sequences (Figure 1). First, we performed the nanosecond-resolved transient absorption measurements under Ar to investigate the kinetics of charge injection, charge recombination, and charge transfer through DNA. The flash excitation of the AQ-moiety led to the formation of  $AQ^{\bullet+}$  with an absorption peak at 530 nm immediately after the flash ( $<10$  ns), demonstrating the injection of a positive charge into DNA (Figure 1A). While  $AQ^{\bullet+}$  decayed rapidly for both full matched and mismatched DNA (Figure 1B, C, D), marked formation of a long-lived charge-separated state was observed for the matched target and probe strands combinations (**I-pT/I-tA**, **I-pC/I-tG**, **II-pA/II-tT**, **II-pG/II-tC**, **III-pC/III-tG**, **III-pT/III-tA**). Thus, competing with the rapid charge recombination, a positive charge migrates across the SNP site more efficiently for fully matched DNA than for mismatched DNA, to be trapped at Z, forming a long-lived charge-separated state, the lifetime of which is longer than  $50 \mu s$ . In the presence of  $O_2$  and  $I^-$ , the long lifetime of the charge-separated state allows the reaction between  $AQ^{\bullet+}$  and  $O_2$  and that between  $Z^+$  and  $I^-$  to proceed, resulting in a complete recovery of the functionalized DNA.

Next, photoirradiation of DNA was performed in the presence of SOD, KI, and starch under air to examine whether functionalized DNA can catalytically produce  $I_2$  upon photoirradiation. Photoirradiation of the fully matched duplex formed between

the probe and the target led to the formation of the absorption of the iodine–starch complex with a peak at around 550 nm (Figure 2A). Of special interest, the concentration of  $I_2$  became higher than  $100 \mu M$  during the photoirradiation of  $1 \mu M$  **I-pA/I-tA**, clearly showing the catalytic production of  $I_2$  (Figure 2B).  $I_2$  production efficiency was markedly decreased for the combination of the probe and the target which forms a mismatch (Figure 2C–E, Table 1). These results clearly demonstrate that SNPs can be detected by monitoring the production yield of  $I_2$  during the photoirradiation of the functionalized DNA.

Finally, in order to verify that this method is capable of detecting SNPs from the small amount of DNA that would be taken from a human being, we examined the detection of SNPs starting from  $0.2 \mu g$  of DNA (Figure 3). Asymmetric PCR was performed in the presence of the triphosphate derivative of D (dDTP) instead of dATP to amplify the single-stranded target of rs965513 (see Supporting Information Figure S3). After removing the dNTPs and DTT included in the PCR buffer solution using spin columns, SOD, starch, and KI were added to the PCR amplicon. The color of the solution turned to blue-purple during photoirradiation for the matched probe and target combinations, while the addition of the probe that forms a mismatch did not cause a significant color change. Even though the color difference between the matched and mismatched DNA was the smallest for rs965513 among the three SNPs sequences studied in the present manuscript (Table 1), the color change of the solution was readily detected by the naked eye, making it possible to detect SNPs without using any special instruments.

The schematic representation of the kinetics of the present photocatalytic  $I_2$  production chemistry is summarized in Figure 4. Although the production yield of  $I_2$  during UV irradiation actually differs between the target solution supplemented with a matched probe and that supplemented with a mismatched probe (Figure 2C–E), the production yield of  $I_2$  was somewhat

(44) Gudbjartsson, D. F.; et al. *Nat. Genet.* **2009**, *41*, 342.

(45) Gudmundsson, J.; et al. *Nat. Genet.* **2009**, *41*, 460.

(46) Sulem, P.; et al. *Nat. Genet.* **2009**, *41*, 734.

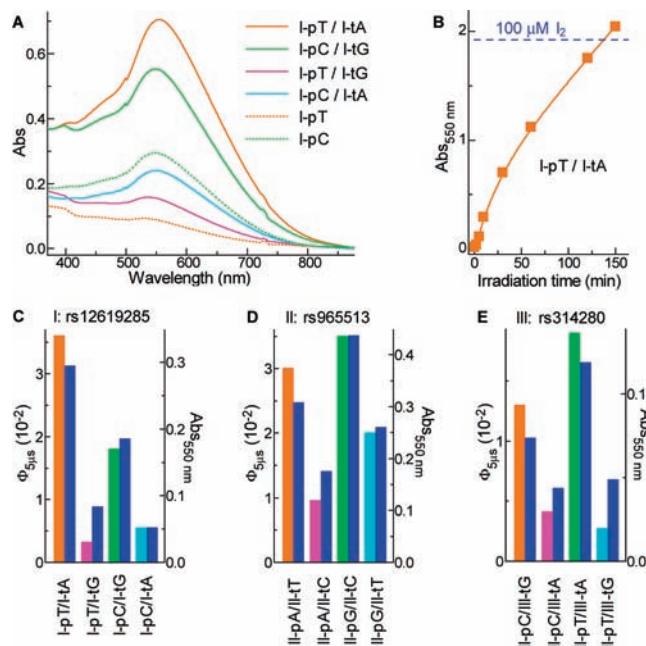


**Figure 2.** Detection of SNPs in the three genomic DNA sequences based on the iodine–starch reaction. (A) Absorption spectra measured after 30 min UV irradiation ( $>340$  nm,  $0.6$  W/cm $^2$ ) under air for the target and probe combinations and for the probe alone for rs12619285. Photoirradiation of the matched duplex formed between the probe and target combination led to the formation of the absorption of the iodine–starch complex, while the  $I_2$  production efficiency was markedly decreased for the combination of the probe and the target that formed a mismatch and in the absence of the target. (B) Time-dependent formation of  $I_2$  during the UV irradiation of **I-pT/I-tA** monitored by absorption at  $550$  nm ( $Abs_{550\text{ nm}}$ ), which clearly demonstrates the photocatalytic formation of  $I_2$ . The horizontal dotted line represents the  $Abs_{550\text{ nm}}$  measured for the  $100\ \mu\text{M}$   $I_2$  solution. (C) Comparison of charge-separation yields ( $\Phi_{5\mu\text{s}}$ ) and formation yields of  $I_2$  monitored by  $Abs_{550\text{ nm}}$  after 10 min of UV irradiation. The  $\Phi_{5\mu\text{s}}$  correlated well with  $Abs_{550\text{ nm}}$ , showing that  $I_2$  is produced via formation of the long-lived charge-separated state in DNA. The sample aqueous solution contained  $1\ \mu\text{M}$  DNA,  $50\ \text{mM}$  KI,  $0.25\%$  starch,  $10\ \mu\text{M}$  SOD in  $10\ \text{mM}$  Na phosphate buffer (pH 7.0). Relatively low DNA concentration was used compared to that used in the transient absorption measurements to check the sensitivity of the present SNP detection system.

**Table 1.** Time Constants for Initial Charge Recombination ( $\tau$ ),<sup>a</sup> Quantum Yields of the Formation of Long-Lived Charge-Separated State Measured at  $5\ \mu\text{s}$  ( $\Phi_{5\mu\text{s}}$ ),<sup>a</sup> and Absorption of the Iodine–Starch Complex Monitored at  $550\ \text{nm}$  ( $Abs_{550}$ )<sup>b</sup>

SNPs	probe/target	$\tau$ ( $\mu\text{s}$ ) <sup>a</sup>	$\Phi_{5\mu\text{s}}$ (%) <sup>a</sup>	$Abs_{550}$ <sup>b</sup>
rs12619285	<b>I-pT/I-tA</b>	0.31	3.6	0.29
	<b>I-pT/I-tG</b>	0.25	0.32	0.083
	<b>I-pC/I-tG</b>	0.31	1.8	0.19
	<b>I-pC/I-tA</b>	0.27	0.55	0.051
rs965513	<b>II-pA/II-tT</b>	0.32	3.0	0.31
	<b>II-pA/II-tC</b>	0.42	0.95	0.18
	<b>II-pG/II-tC</b>	0.32	3.5	0.44
rs314280	<b>III-pC/III-tT</b>	0.33	2.0	0.26
	<b>III-pC/III-tG</b>	0.27	1.3	0.073
	<b>III-pC/III-tA</b>	0.34	0.41	0.044
	<b>III-pT/III-tA</b>	0.27	1.9	0.12
	<b>III-pT/III-tG</b>	0.31	0.27	0.048

<sup>a</sup> Initial charge-recombination rate ( $1/\tau$ ) and charge-separation yield of the long-lived charge-separated state monitored at  $5\ \mu\text{s}$  ( $\Phi_{5\mu\text{s}}$ ) were determined from the single exponential fit of the time profile of the decay of  $AQ^{\cdot-}$  shown in Figure 1. <sup>b</sup> The formation yields of  $I_2$  monitored by absorption at  $550\ \text{nm}$  ( $Abs_{550\text{ nm}}$ ) after 10 min of UV irradiation. The sample aqueous solution contained  $1\ \mu\text{M}$  DNA,  $50\ \text{mM}$  KI,  $0.25\%$  starch,  $10\ \mu\text{M}$  SOD in  $10\ \text{mM}$  Na phosphate buffer (pH 7.0).

low for some matched probe–target combinations. This is because the charge-transfer efficiency and the subsequent

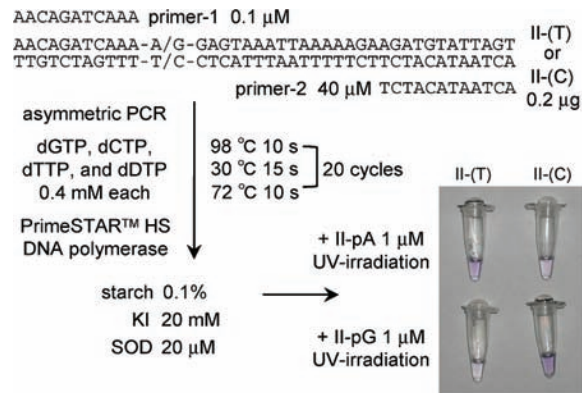


**Figure 3.** Detection of SNPs from a small amount of genomic DNA sequences based on the iodine starch reaction. Asymmetric PCR was performed to amplify  $0.2\ \mu\text{g}$  of genomic sequences rs965513 (**II-(T)** and **II-(C)**). dNTPs and DTT included in the PCR buffer solution were removed using spin columns, and then Na phosphate buffer (pH 6.0), SOD, KI, and probe DNA were added to the PCR tube and UV-irradiated for 150 min ( $>340$  nm,  $0.07$  W/cm $^2$ ). The color of the solution turned to blue-purple during photoirradiation for the probe and target combinations that formed a matched duplex, while the probe and target combinations that formed a mismatch did not cause a significant color change.

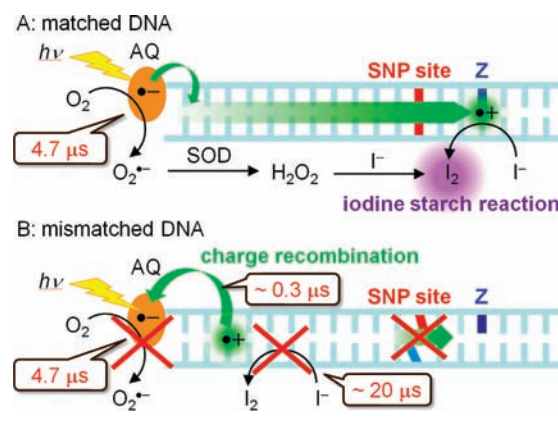


**Figure 4.** Schematic representation of the kinetics of charge injection, charge recombination, and generation of  $I_2$  in (A) matched and (B) mismatched DNA. (A) Long-lived charge-separated state ( $\tau > 50\ \mu\text{s}$ ) forms for matched DNA which allows the reaction between  $AQ^{\cdot-}$  and  $O_2$ , and reaction between  $I^-$  and  $Z^+$  to eventually form  $I_2$ . (B) In the presence of a mismatch, charge-recombination proceeds rapidly ( $\sim 0.3\ \mu\text{s}$ ) which prohibits the reaction between  $AQ^{\cdot-}$  and  $O_2$  ( $4.7\ \mu\text{s}$ ), and reaction between  $I^-$  and  $D^+$  or  $G^+$  ( $\sim 20\ \mu\text{s}$ ).

formation yield of  $I_2$  differ from sequence to sequence. The production yield of  $I_2$  became low when the charge-transfer rate through DNA was not fast enough to effectively compete with the charge recombination. We previously reported that a positive charge moves faster through DNA having A-T base-pairs replaced with deazaadenine-T base-pairs than through DNA having A-T base-pairs replaced with D-T base-pairs.<sup>26,27</sup> The development of a DNA polymerase which can fully incorporate the triphosphate analogue of deazaadenine may allow further improvement of the present SNPs detection system. The generation of  $I_2$  was observed to some extent for the single-stranded probe **I-pC** (Figure 2A). In such cases, the probe DNA could be further refined by changing the relative positions of the AQ and Z to the SNPs site to avoid the intrastrand charge-separation process.

The elucidation and refinement of the charge-transfer kinetics through DNA allowed us to develop a functionalized DNA system which can convert photon energy into chemical energy

stored in I–I covalent bonds. The production yield of I<sub>2</sub> was significantly affected by the presence of a mismatch in DNA that blocked a charge-transfer process, which enabled the detection of SNPs in the genomic sequences by the naked eye through a color change during the iodine starch reaction. The present system may also be applicable for monitoring interactions such as that between the aptamer and the target molecule<sup>47</sup> and that between a protein and DNA,<sup>48</sup> both of which were reported to affect the charge-transfer kinetics in DNA.

**Acknowledgment.** We thank Prof. K. Nakatani of SANKEN for the MALDI mass measurement. This work has been partly supported by a Grant-in-Aid for Scientific Research (Projects

(47) Sankar, C. G.; Sen, D. *J. Mol. Biol.* **2004**, *340*, 459.

(48) Nakatani, K.; Dohno, C.; Ogawa, A.; Saito, I. *Chem. Biol.* **2002**, *9*, 361.

22245022 and 21750170) from the MEXT of Japanese Government, and by grants from the Association for the Progress of New Chemistry (to K.K.). T.M. thanks the WCU (World Class University) program through the National Research Foundation of Korea funded by the Ministry of Education, Science and Technology (R31-10035) for support.

**Supporting Information Available:** DNA synthetic procedures, MALDI-mass of DNA studied, measurement of the rate constant of the reaction between AQ<sup>•-</sup> and O<sub>2</sub>, and that between I<sup>-</sup> and a positive charge generated in DNA, and native agarose gel analysis of PCR products. Complete refs 44, 45, and 46 in this document as refs 2, 3, and 4. This material is available free of charge via the Internet at <http://pubs.acs.org>.

JA105850D